Limnol. Oceanogr., 58(3), 2013, 893–902

doi:10.4319/lo.2013.58.3.0893

Assessment of light absorption within highly scattering bottom sea ice from under-ice light measurements: Implications for Arctic ice algae primary production

Jens K. Ehn* and C. J. Mundy

Centre for Earth Observation Science, University of Manitoba, Winnipeg, Manitoba, Canada

Abstract

Primary production estimates of ice algae within the bottommost layers of the Arctic ice cover are commonly derived using irradiance measurements taken immediately below the solid ice bottom. However, radiation absorbed by ice algae is significantly affected by the high-scattering sea ice environment they are embedded within because scattering increases the pathlength traveled by photons and therefore the probability of photon encounters with algal cells. Failing to account for this enhanced absorption may considerably affect estimates of the timing and magnitude of ice algal production. To demonstrate the effect of scattering and attenuation, multipliers for absorption amplification (Φ) and layer average opacity (χ) were derived from observations of chlorophyll *a* concentration and the vertical attenuation coefficient over the bottom 2.5 cm of landfast sea ice. Φ reached values over 19 at low chlorophyll *a*, but became < 2 at high biomass levels, whereas χ became larger as biomass levels increased. Using Φ to construct an apparent photosynthesis vs. irradiance relationship showed that light limitation is greatly reduced relative to the case where scattering is not considered. This highlights an important interaction not previously noted for ice algal production in their high-scattering environment. Knowledge of this absorption amplification can help explain ice algal phenology during the spring bloom and will improve ice algal production estimates and model parameterizations.

The Arctic ice-covered marine environment is rapidly changing with recent accelerated declines in sea ice cover (Comiso et al. 2008) and consistent disappearance of old (thick) multiyear ice (Maslanik et al. 2007). These changes will have an effect on the polar marine ecosystem; however, the extent of this effect and future changes on the ecosystem are not well understood. Modeling variability and environmental change in polar marine ecosystems is therefore critically important.

A key ecological component of the Arctic ice cover is the spring bottom ice algal bloom, which provides an initial food source when phytoplankton growth is at a minimum (Gosselin et al. 1997). Ice algae predominantly reside within a few-centimeters-thick layer at the bottom of Arctic sea ice (Welch and Bergmann 1989). During commencement of the spring bloom, bottom ice algal growth is light limited due to both low diurnal solar insolation during late winter and early spring and the strong attenuation of light as it is transmitted through the snow and sea ice. Thus, determining the amount of solar energy absorbed in the ice algae layer is of significant importance for predicting the seasonal development of the sea ice algae.

The photosynthesis vs. irradiance (*P*-*E*) relationship provides insight into the physiology of photosynthetic organisms (Falkowski and Raven 2007), including its use to estimate light limitation in ice algal growth models (Arrigo et al. 1993; Lavoie et al. 2005; Nishi and Tabeta 2005). *P*-*E* relationships are usually measured using algae suspended in water where scattering is low compared to that of sea ice, and absorption by algal cells is directly obtained as the product of measured algal absorption coefficient, a_ϕ ($\mathrm{m^{-1}}$), and scalar irradiance, E_0 ($\mu\mathrm{mol\ m^{-2}\ s^{-1}}$). Measurements on ice algae are no exception, having been made on melted ice (Kirst and Wiencke 1995) or extracted brine samples (Ralph et al. 2005; Manes and Gradinger 2009), whereas the number of in situ studies remains limited (Mock and Gradinger 1999; McMinn et al. 2000; Kühl et al. 2001).

Since sea ice is a solid material, it is not easy, nor practical, to measure E_0 within the ice matrix without disturbing the light field. Typically, E_0 has thus been estimated from measurements below the ice (Smith et al. 1988). An alternative approach is to calculate the amount of solar radiation absorbed within a layer of sea ice from net (downward) irradiances using the principle of energy conservation, analogous to calculating the radiative heating rate (Ohlmann et al. 2000). Here we compare these two approaches of estimating radiant energy absorption in the bottom ice algal layer and demonstrate a large discrepancy in their result. Finally, we discuss steps to estimate photosynthetically active radiation (PAR) levels within the ice algae layer from measurements taken immediately beneath the ice cover and examine the effects of these estimates on primary production in sea ice due to enhanced solar absorption caused by scattering in the ice algal layer.

Methods

Solar radiant energy absorbed in sea ice bottom layer—To directly utilize the product $a_\phi E_0$ to calculate the radiation absorbed by ice algae embedded within the bottommost few centimeters of the sea ice cover, light measurements have been conducted directly beneath the sea ice cover and applied to estimate E_0 values within the ice (Smith et al. 1988; Mock and Gradinger 1999). Following Smith et al. (1989), an average scalar irradiance ($\bar{E}_0$) for the bottom ice algal layer of thickness (h_ϕ) has been calculated as:

---

* Corresponding author: jens_ehn@umanitoba.ca

$$\bar{E}_0 = \frac{\int_0^{h_\phi} E_{0bot}\, e^{K_0 z} dz}{h_\phi} = \frac{E_{0bot}\,(e^{K_0 h_\phi}-1)}{K_0 h_\phi} \tag{1}$$

where $K_0 = ln[E_{0top}\, E_{0bot}^{-1}]\, h_\phi^{-1}$ is the scalar diffuse attenuation coefficient (m^{-1}), and E_{0top} and E_{0bot} are scalar irradiances at the top and bottom interfaces of the layer, respectively. However, as shown below, Eq. 1 is not consistent with the law of radiant energy conservation in a scattering volume.

A second approach begins with the principle of energy conservation for a layer expressed in the form of the one-dimensional Gershun's equation:

$$\frac{dE}{dz} = -a_{\mathrm{tot}} E_0 \tag{2}$$

where a_{tot} is the total absorption coefficient (m^{-1}) and $dE{:}dz$ the depth derivate of net (downward) irradiance (μmol m^{-2} s^{-1}) with the depth z positive downwards. Equation 2 is exact when no internal sources of radiation are present. An estimate of the average scalar irradiance ($\hat{E}_0$) within the ice algae layer can be obtained for a discrete thickness h_ϕ, by rearranging Eq. 2 so that

$$\hat{E}_0 = \frac{1}{a_{\mathrm{tot}}}\frac{\Delta E}{\Delta z} = \frac{E_{bot}(e^{K_{\mathrm{E}} h_\phi}-1)}{a_{\mathrm{tot}} h_\phi} \tag{3}$$

where $K_{\mathrm{E}} = \ln(E_{top}\, E_{bot}^{-1}) h_\phi^{-1}$ is the net irradiance attenuation coefficient (m^{-1}), and E_{top} and E_{bot} are net irradiances at the top and bottom layer interfaces, respectively.

We have thus determined the layer average scalar irradiance from measurements at the layer bottom interface in two ways, first $\bar{E}_0$ using Eq. 1 and then $\hat{E}_0$ using Eq. 3. In non-scattering media or when scattering is negligible compared to absorption, Eq. 1 and Eq. 3 are equivalent; however, as scattering increases, $\hat{E}_0 > \bar{E}_0$, since $K_0 > a_{\mathrm{tot}}$, even though $\Delta E < \Delta E_0$. However, the magnitude of this difference in a high-scattering environment such as sea ice and its effects have not been considered before.

Application to the bottom ice algae layer—Here we describe how the parameters in Eq. 1 and Eq. 3 were estimated in order to evaluate $\bar{E}_0$ and $\hat{E}_0$ as a function of chlorophyll *a* (Chl *a*) concentration within the bottom ice algal layer using values found in literature. Chl *a* is the main photosynthetic pigment in algae and thus commonly used as a proxy for autotrophic biomass.

Ice algal layer PAR transmittance with coincident determination of Chl *a* has been measured in situ by Welch and Bergmann (1989), Mundy et al. (2007), and Ehn et al. (2008*a*). These data allowed for determination of the downwelling PAR attenuation coefficient, K_{d} (m^{-1}), for h_ϕ = 0.025 m with areal Chl *a* ranging from 0.8 to 135 mg m^{-2} (32 to 5400 mg m^{-3}; Fig. 1).

We fitted this K_{d}(PAR) against Chl *a* using a robust nonlinear least-squares regression with a model of the form

$$K_{\mathrm{d}}(\mathrm{PAR}) = -\frac{1}{h_\phi}\ln\left(\int_{400}^{700} E_{\mathrm{d}top}(\lambda)\, e^{-K_{\mathrm{d}}(\lambda) h_\phi} d\lambda \left[\int_{400}^{700} E_{\mathrm{d}top}(\lambda) d\lambda\right]^{-1}\right) \tag{4a}$$

where

$$K_{\mathrm{d}}(\lambda) = \frac{1}{\mu_{\mathrm{d}}}\left[\left(a_{\mathrm{ice}}(\lambda)+a_{\mathrm{p}}(\lambda)\right)^2 + 0.238\left(a_{\mathrm{ice}}(\lambda)+a_{\mathrm{p}}(\lambda)\right) b_{\mathrm{tot}}\right]^{0.5} \tag{4b}$$

μ_{d} is the average cosine of the downwelling hemisphere of the light field (dimensionless), $E_{\mathrm{d}top}(\lambda)$ is the downwelling irradiance at the top of the algae layer, $K_{\mathrm{d}}(\lambda)$ the downwelling diffuse attenuation coefficient, and $a_{\mathrm{ice}}(\lambda)$ and $a_{\mathrm{p}}(\lambda)$ are the pure sea ice and algal absorption coefficients (m^{-1}) for the bottom ice algal layer (Fig. 2). The sum of a_{ice} and a_{p} is a_{tot}. For the purpose of this study, additional contributions to absorption by colored dissolved organic matter were assumed negligible relative to algal absorption in the bottom ice algal community as has been previously observed (Ehn et al. 2008*a*). The unknown in Eq. 4b, b_{tot}, represents the total volume scattering coefficient for the ice (m^{-1}) and is assumed to be spectrally independent over PAR wavelengths because the inclusions dominating scattering in sea ice are much larger than the wavelength of light (Perovich 1990). Equation 4b has the form of the numerically generated equation developed by Kirk (1994), and has been shown to be appropriate for sea ice and turbid waters (Maffione 1998). The Chl *a*–specific spectral absorption coefficients for ice particulate matter, $a^*_{\mathrm{p}}(\lambda)$ (and also for algal pigments, $a^*_\phi(\lambda)$, after methanol extraction), obtained through linear least-squares regression of 23 ice algae spectra against their Chl *a* concentrations that ranged from 0.48 to 1080 mg m^{-3} ($r^2 > 0.97$ over PAR wavelengths) was used to determine $a_{\mathrm{p}}(\lambda)$. These ice algae data were collected during spring 2008 in the southern Beaufort Sea as a part of the International Polar Year–Circumpolar Flaw Lead study (Mundy et al. 2011). Pure ice spectral absorption from Grenfell and Perovich (1981) was used for $a_{\mathrm{ice}}(\lambda)$, and μ_{d} was set to a constant 0.7 based on observations and modeling of Ehn et al. (2008*a*,*b*). This μ_{d} is similar to that of Arrigo et al. (1991), and others since, who used a constant value of 0.656 for all depths within the ice cover.

Spectral weighting for PAR integrations was provided by a downwelling irradiance spectrum transmitted through an ice cover with a 37.8 cm snow cover, 1.3 m ice thickness, and only 0.4 mg Chl *a* m^{-2} reported by Mundy et al. (2007; *see* their fig. 3a). The sea ice conditions and geographical location in that study were similar to those in Welch and Bergmann (1989). Furthermore, the spectral shapes of the transmitted irradiance remained almost identical (although magnitudes varied) for all low Chl *a* concentrations even as snow and ice thickness varied. Therefore, the irradiance spectrum can be considered appropriate for spectral weighting purposes just above the ice algae layer, i.e., $E_{\mathrm{d}top}$ in Eq. 4a.

Fitting Eq. 4 to the data (Fig. 1) resulted in a b_{tot} value of 295.4 m^{-1} that was within the range of scattering coefficients (165 to 431 m^{-1}) previously estimated for bottom sea ice (Ehn et al. 2008*a*). However, we emphasize that b_{tot} is simply a fitting parameter that depends on other

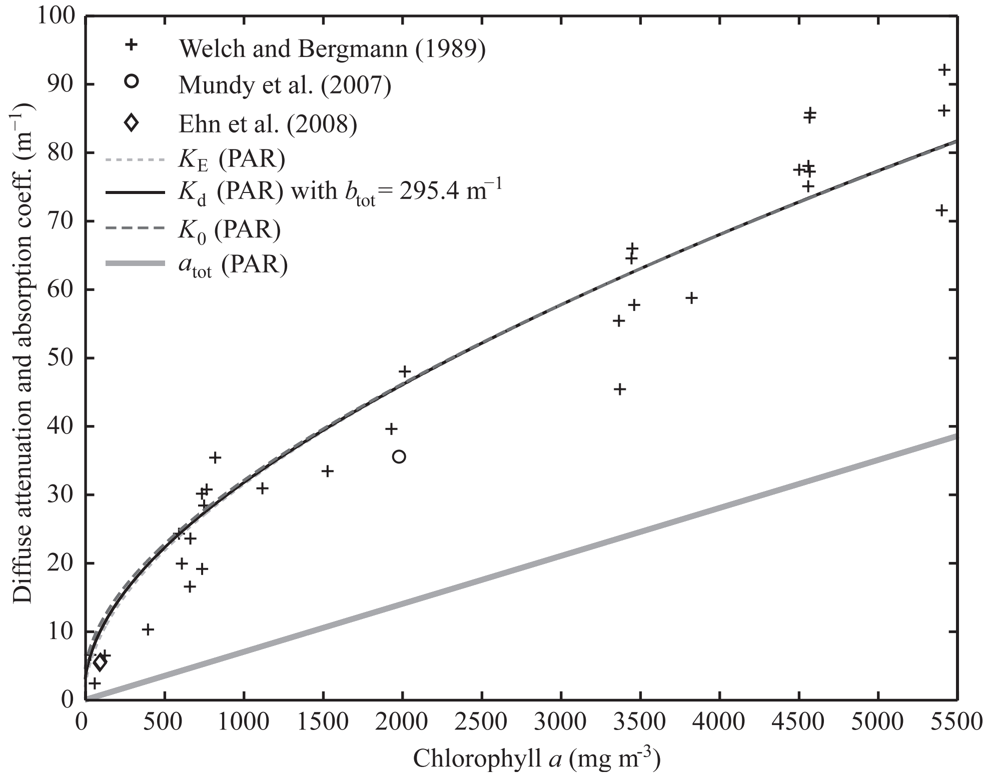

Fig. 1. Observed (symbols) and best-estimate ($r^2 = 0.94$, root mean square error = 6.86, $n = 36$) of the bottom ice algal layer diffuse attenuation coefficients, K_d (Eq. 4), K_E, and K_0, and absorption coefficient (coeff.), a_{tot}, as functions of Chl *a*. The crosses represent K_d over the bottom 2.5 cm of the sea ice calculated using data from Welch and Bergmann (1989) (*see* their fig. 2) with one outlier (632 mg m^{-2}, 2.3 m^{-1}) removed. The circle and diamonds were calculated from Mundy et al. (2007) and Ehn et al. (2008*a*), respectively.

values chosen in Eq. 4, and the resultant K_d represents a fit to observed data from natural sea ice.

Net and scalar irradiance estimation—Equation 4b was used to estimate the downwelling irradiance spectra of the lower layer interface, $E_{dbot}(\lambda)$, from the irradiance, $E_{dtop}(\lambda)$, at the upper interface of the 2.5 cm thick ice algal layer. The corresponding upwelling irradiances, $E_{utop}(\lambda)$ and $E_{ubot}(\lambda)$, needed to be estimated to determine the scalar and net irradiances and attenuation coefficients in Eqs. 1 and 3, respectively (Fig. 3). The bottom ice algal layer is located in the bottom few centimeters of sea ice at the ice–water interface, below which scattering in seawater is orders of magnitude smaller than within the ice matrix, resulting in $E_u \ll E_d$ (Grenfell 1979; Light et al. 2008). We followed Morel and Maritorena (2001) and calculated the reflectance at the ice–ocean interface, R_{bot} ($= E_{ubot} : E_{dbot}$), as

$$R_{bot}(\lambda) = 0.33 \frac{b_{bbot}(\lambda)}{a_{sw}(\lambda) + b_{bbot}(\lambda)} \tag{5}$$

where b_{bbot} and a_{sw} are the backscattering and absorption coefficients of the under-ice seawater layer, respectively (Fig. 4). We assumed an arbitrary low value of 0.01 mg m^{-3} for the seawater Chl *a* concentration, and obtained b_{bbot} as $0.5(1.29/\lambda)^{4.32} + b_{bp}$, where the particulate backscattering coefficient, b_{bp}, was calculated according to Eq. 10 in Morel and Maritorena (2001) as a function of Chl *a*. The seawater absorption was calculated as the sum of the pure seawater absorption and phytoplankton absorption (which assumed that $a_p^*(\lambda)$ for ice algae was valid also for the under-ice water column).

Reflectance within the bottom layers of sea ice is not well known but expected to vary strongly with changes in ice algae biomass levels. Upwelling and downwelling irradiance profiles in clean ice obtained by Light et al. (2008) with a Monte Carlo model suggest that R_{top} (2.5 cm above the ice bottom) at 500 nm was close to 4%. This may be the only published estimate of upwelling irradiance in bottom layers of sea ice. Such a low value indicates that the bottom 2.5 cm layer is optically thin when the biomass concentration is low. Therefore, upwelling from the seawater below also influences R_{top}. We thus applied the formulation for diffuse reflectance from oceanic shallow waters by Maritorena et al. (1994):

$$R_{top}(\lambda) = \frac{b_b}{(1+\mu_d \mu_u^{-1})K_d} + \left(R_{bot} - \frac{b_b}{(1+\mu_d \mu_u^{-1})K_d}\right) e^{-\left(1+\mu_d \mu_u^{-1}\right) K_d h_\phi} \tag{6}$$

where μ_u is the upwelling average cosine and was set to a constant 0.5, i.e., a diffuse upwelling light field. The value

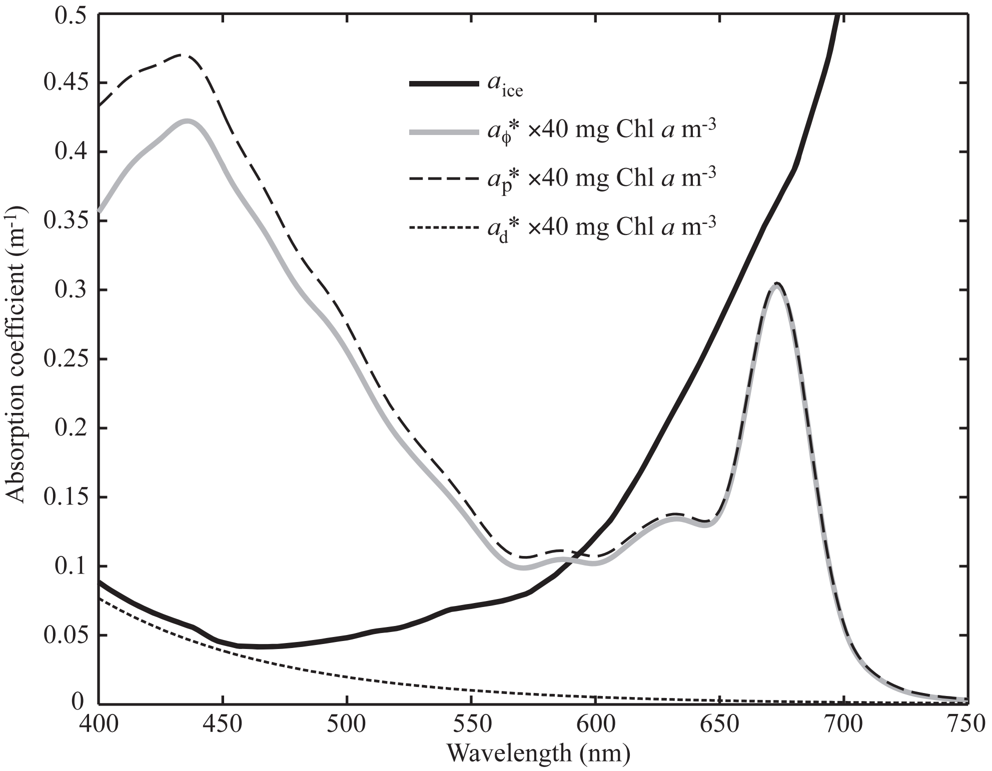

Fig. 2. Pure ice absorption spectrum (Grenfell and Perovich 1981) and Chl *a* (determined fluorometrically)–specific spectral absorption coefficients for algal particulates, $a^*_\mathrm{p}(\lambda)$, their pigments, $a^*_\phi(\lambda)$, and de-pigmented matter, $a^*_\mathrm{d}(\lambda)$ multiplied by 40 mg Chl *a* m^{-3}.

for b_b, the backscattering coefficient of the ice algae layer, was set to $0.00437 b_\mathrm{tot}$, implying that 0.437% of the scattered photons were backscattered, which gives an R_{top} of 4% at 500 nm when Chl *a* concentration is zero. Such a value corresponds to an average cosine of the scattering angle of about 0.98 for a scattering phase function by Henyey and Greenstein (1941). Spectra of R_{top} and R_{bot} are shown in Fig. 4a.

Scalar and net irradiances at the layer interfaces (subscript *n* is either *top* or *bot*) were then calculated as

$$E_{0n} = \frac{E_{\mathrm{d}n}}{\mu_{\mathrm{d}n}} + \frac{E_{\mathrm{u}n}}{\mu_{\mathrm{u}n}} \tag{7}$$

and

$$E_n = E_{\mathrm{d}n} - E_{\mathrm{u}n} \tag{8}$$

respectively (Fig. 3).

The spectral net irradiances normalized to an $E_{\mathrm{d}top}$ (PAR) = 1, and that correspond to reflectances, are shown in Fig. 4b. As the absorption by ice algae increases in the bottom layer, E_{bot} decreases and its peak magnitude is shifted from 450–500 nm to 560–570 nm. E_{top} shows a smaller increase with increasing Chl *a* as $E_{\mathrm{u}top}$ is reduced from the algae layer due to absorption. Both R_{top}(PAR) and R_{bot}(PAR) decrease with Chl *a* (not shown). However, in the case of R_{bot}(PAR), the decrease is solely due to changes in the spectral shape of the irradiance transmitted through the ice algae layer, which affects the weighting of the PAR integration (the spectral $R_{bot}(\lambda)$ remained constant as in Fig. 4a).

Results

PAR estimation for ice algae layer from under-ice measurements—The two approaches to estimating the solar energy absorbed by the ice algae layer were found to differ so that the product $a_\mathrm{tot}\bar{E}_0$ (Eq. 1) significantly underestimated what was absorbed by the ice algae layer compared to $\Delta E : \Delta z$ (Eq. 3). In general, $K_0 > K_\mathrm{d} > K_\mathrm{E}$; however, the difference between them is minimal compared to the much smaller a_tot (Fig. 1) resulting in the difference between $\hat{E}_0$ and $\bar{E}_0$. To illustrate this discrepancy, we define an absorption amplification factor (Φ) as

$$\Phi = \frac{\hat{E}_0}{\bar{E}_0} \tag{9}$$

Similarly, to show the difference to scalar irradiance transmitted through the ice bottom, which is readily measurable, we define a layer average opacity factor (χ) as

$$\chi = \frac{\bar{E}_0}{E_{0bot}} \tag{10}$$

Fig. 5a shows that in the high-scattering sea ice environment, scattering dominates at low Chl *a*, causing Φ(PAR) to increase to a maximum of ~ 19.3. However, at high Chl *a*, absorption increases in importance and Φ approaches unity.

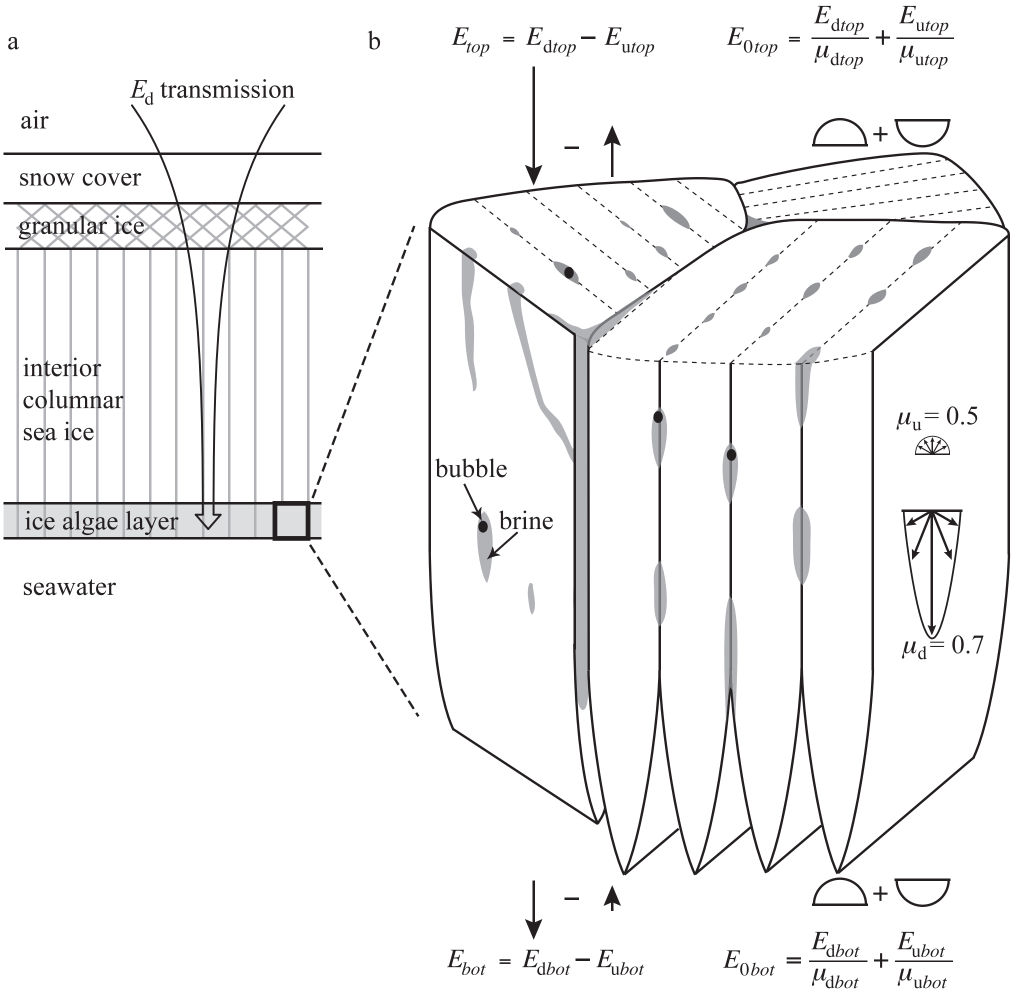

Fig. 3. Schematic of typical structure and texture of (a) level sea ice and (b) the bottom skeletal layer where most ice algae are found. The arrows summarize the various radiation fields pertinent to this study (*see* text).

The Φ(PAR) calculated from PAR integrated irradiances is hereafter referred to as Φ for brevity, while spectral Φ(λ) are shown in Fig. 5b for selected Chl *a* concentrations. The behavior of Φ as a function of Chl *a* (mg m^{-3}) can be parameterized as $[1 + 7199(18.74 + \text{Chl } a^{0.9302})^{-1}]^{0.5}$ ($r^2 > 0.999$). To estimate the average scalar irradiance received by the ice algae from readily obtainable sub-ice measurements, E_{0bot} must be multiplied by both χ and Φ. For pure ice without algae, χ is close to unity, and as Chl *a* increases, χ can be parameterized as $\exp[0.0001163(\text{Chl } a^2 + 12{,}490\text{Chl } a)^{0.5}]$ ($r^2 > 0.999$). The product $\chi\Phi$ obtains a minimum at a Chl *a* around 2400–2800 mg m^{-3}, above which absorption by algae becomes more important than absorption amplification by scattering in determining the light level in the bottom ice algal layer.

Sensitivity analysis and ranges—A main uncertainty affecting Φ is the absence of detailed information in the literature on the angular distribution of the light field within sea ice. Eq. 2 shows that the radiation absorption within a layer is determined by the vertical flux divergence, dE/dz, where both the downwelling and upwelling radiation fields, E_d and E_u, are needed to determine E. Generally, E_u is expected to attenuate more strongly than E_d due to a more horizontally oriented radiance distribution.

To describe the angular distribution of the light field, we have used a constant μ_u of 0.5 vs. a μ_d of 0.7. These values are currently uncertain as they have never been determined through experiments. However, the shape of the light field can be expected to remain fairly constant during natural conditions when the vernal bottom ice algae blooms are initiated for various reasons. Seasonal ice in the Arctic has reached its maximal thickness of 1–2 m during spring and is typically covered by highly scattering freeboard layers. Therefore, the ice is optically thick such that the penetrating solar radiation reaches an asymptotic state, i.e., the shape of the radiation field does not change with depth, within the inner portion of the sea ice cover (Ehn et al. 2008*b*). Thus, the shape of the radiation field is not expected to have a high degree of variability from place to place. Approaching the ice bottom, the radiation field becomes increasingly influenced by the differing optical properties (particularly the sharp reduction in scattering) of the underlying water column. However, this boundary effect should be very consistent for typical level sea ice covers. Reflectance from the underlying seawater is also

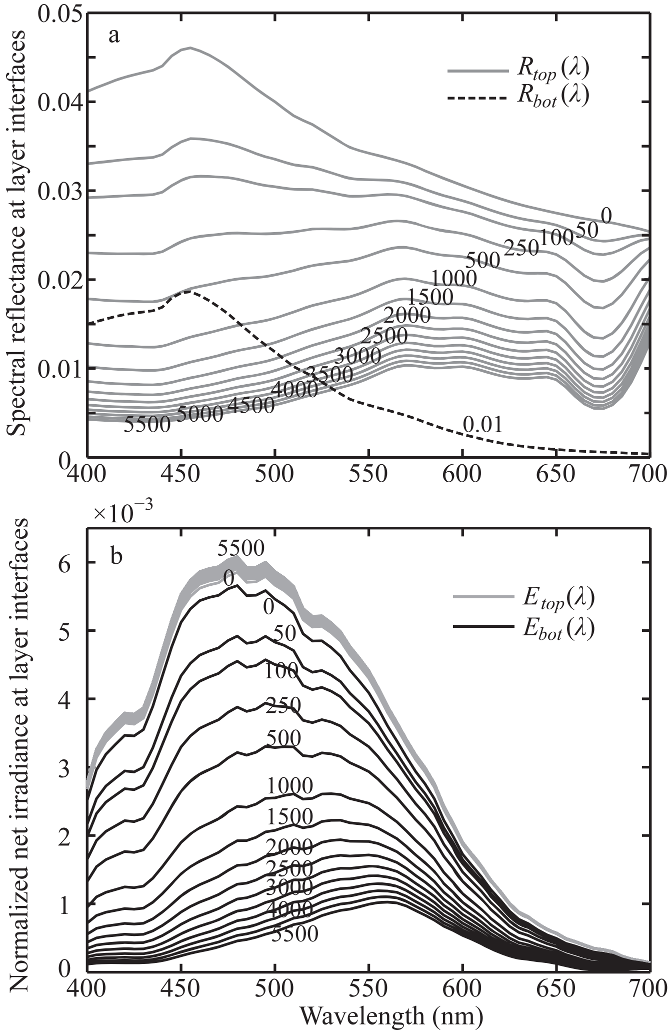

Fig. 4. (a) Spectral reflectances and (b) net irradiances as a function of Chl *a* at the top and bottom interfaces of the ice algae layer.

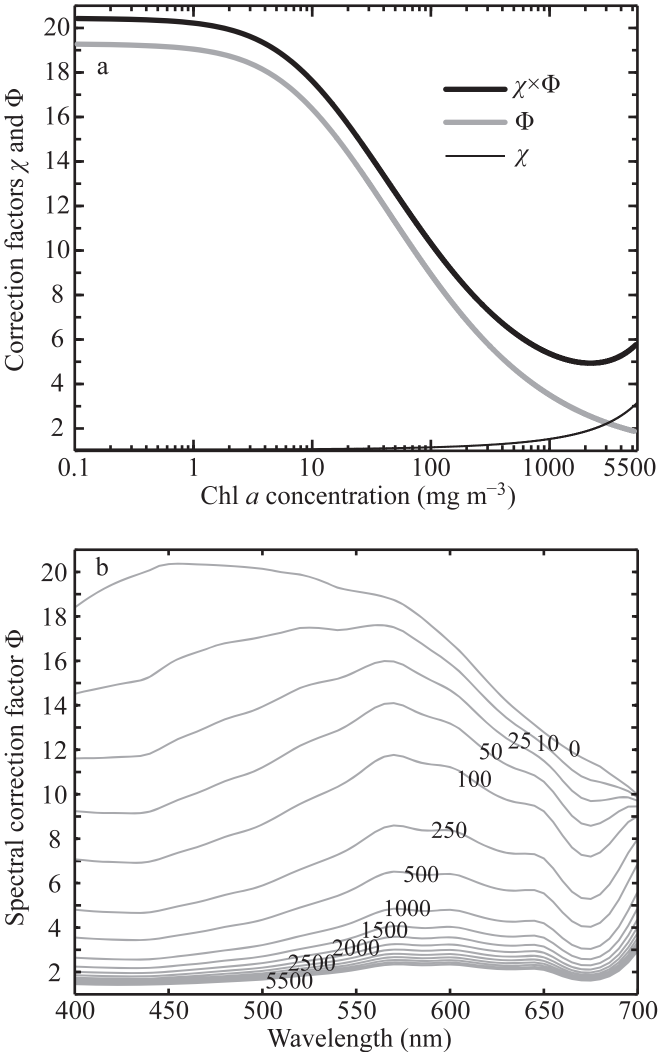

Fig. 5. (a) The correction factors Φ and χ, integrated over PAR, and their product as a function of Chl *a* (*see* Eqs. 7 and 8). In (b) the spectral $\Phi(\lambda)$ over a selected Chl *a* range.

well constrained from numerous studies in open-water environments and can be measured quite accurately due to the lack of waves under sea ice. Furthermore, changes in the seawater reflectance, R_{bot}, will affect R_{top} in the same direction so that the net effect is moderated, especially when Chl *a* is low (*see* Eq. 6). Finally, the structure and properties of the sea ice in the layers near the seawater interface are typically quite similar, i.e., horizontally homogeneous layers of slowly grown sea ice with a columnar type structure and temperatures near the seawater freezing point (Fig. 3). Thus, one can expect similar optical properties of such sea ice.

A maximum amplification factor Φ is obtained when assuming that upwelling radiation is so small that it is negligible and that the downwelling portion is completely downward directed (i.e., $\mu_d = 1$). This results in a maximal Φ of 52 at small Chl *a* and $b_{tot} = 698$ m^{-1} to fit data in Fig. 1. However, this is not a physically realistic scenario since when $\mu = 1$, both $E_d = E_0 = E$ and $K_0 = K_E = a_{tot}$, which means that b_{tot} has to be zero. If the attenuation within the ice algae layer was solely determined by its absorption or the radiation field was fully downward directed with forward scattering, then the data relationship in Fig. 1 would also be expected to increase linearly as a function of algae biomass, which is not the case. When $\mu_d = 0.7$, E_u neglected, and with other values as assumed above, a maximum Φ of 33.9 results. We note, however, that reflectance ($E_u : E_d$) is not negligible in sea ice or even in pure seawater. Nor is it constant with distance into the ice from the ocean interface, and is wavelength dependent since it is inversely proportional to a_{tot}.

Variations in Φ due to variations in the angular radiation distribution over realistic ranges are summarized in Fig. 6. As μ_d is increased (decreased), Φ also increases (decreases) since b_{tot} is adjusted in the fitting of Eq. 4 to data. With $\mu_d = 0.6$, b_{tot} becomes 193.6 m^{-1} and with $\mu_d = 0.8$, b_{tot} is 413.4 m^{-1}, which fits within the range obtained in Ehn et al. (2008*a*). The resultant Φ changes by about ± 4 for a ± 0.1 change in μ_d at low Chl *a*, whereas changes in Φ become smaller at high Chl *a* (Fig. 6). Changes in Φ due to variations in μ_u from 0.2 to 0.6 range about 1.1 maximally

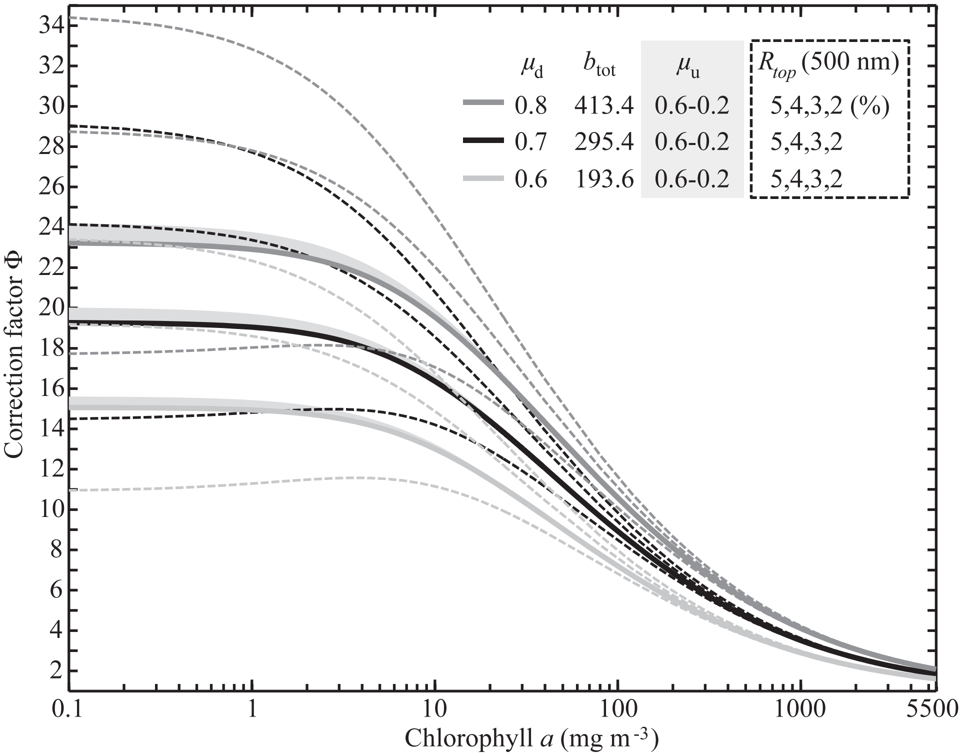

Fig. 6. Variations in Φ due to changes in the angular distribution of the light field and backscattering ratio within the bottom ice algae layer. The three solid lines represent the response to changes in μ_d from 0.6 to 0.8 (with new b_{tot} fittings to match K_d observations using Eq. 4), with surrounding shaded areas representing the response to changes in μ_u from 0.6 (smaller Φ) to 0.2 (larger Φ) with the solid line having $\mu_u = 0.5$. The black solid line is the result shown in Fig. 5. Dashed lines represent changes due to R_{top} with higher values leading to lower Φ. R_{top} was adjusted to fixed values of 5%, 4% (standard case), 3%, and 2% at 500 nm using the backscattering ratio (*see* text).

at low Chl *a*. The largest effect on Φ is due to changes in the backscattering ratio, which results in changes in R_{top} and consequent changes in the net irradiance, E_{top}. At a Chl *a* concentration of 0.1 mg m^{-3}, variations in R_{top}(500 nm) from 2% to 5% resulted in a linear change in Φ of −4.2, −4.9, and −5.6 per percent unit change in R_{top}(PAR) for the three different $\mu_d = 0.6$, $\mu_d = 0.7$, and $\mu_d = 0.8$, respectively (Fig. 6). At higher Chl *a* levels, the magnitude of these slopes are reduced.

We have used a constant $a^*_p(\lambda)$ spectrum that integrated to an a^*_p(PAR) of 0.007 m^2 mg^{-1} to calculate our values. After removing the influence of nonpigmented material, this value corresponds to an a^*_ϕ(PAR) of 0.0064 m^2 mg^{-1} (Fig. 3), which is very close to the 0.006 m^2 mg^{-1} used by Arrigo et al. (1993). However, a change in absorption characteristics of the algae has a significant effect on Φ particularly at low Chl *a* concentrations. A sensitivity analysis of the effect of ice algae absorption when Chl *a* is 0.1 mg m^{-3} or smaller results in a linear decrease of Φ with a slope of −3.75 per every 0.001 m^2 mg^{-1} increase of $a^*_p(\lambda)$ (by multiplier on spectrum), when $\mu_d = 0.7$, $\mu_u = 0.5$, and the b_{tot} tuned by fitting Eq. 4 to data and the $b_b : b_{tot}$ ratio tuned so that R_{top} was 4%. Similarly, when Chl *a* concentrations were 10, 100, 1000, and 5000 mg m^{-3}, the Φ slopes were −2.97, −1.68, −0.63, and −0.26 per 0.001 m^2 mg^{-1} increase in $a^*_p(\lambda)$ magnitude, respectively. This analysis shows that pigment packaging effects that can reduce $a^*_p(\lambda)$ at high Chl *a* will have only a small effect on Φ as values remain relatively small.

Discussion

The theory we presented here represents a first step towards the inclusion of scattering effects on absorption needed in the parameterization of primary production for future polar sea ice ecosystem models and that is consistent with energy conservation over a layer. Mundy et al. (2007) showed that ice algal biomass could be estimated from transmitted light spectra. However, to additionally remotely estimate ice algal primary production, the light levels with the bottom layers of the sea ice need to be assessed. Therefore, we have proposed a framework to correct irradiance measurements taken immediately below the ice cover to better reflect the enhanced radiation absorption within the highly scattering sea ice. More detailed bio-optical observations are required for further improvement and validation of the theory and parameterizations. Areas of improvement include: treatment and measurements of scalar vs. vector irradiance within the sea ice (i.e., accounting for the shape of the light field) and of spectral absorption and transmission, consideration of an algal pigment packaging effect, improvement of scattering parameterizations for the bottom ice skeletal layer and algal cells, in particular scattering from the siliceous frustules of diatoms (Ehn et al. 2008*a*), and improved observations of the bottom ice skeletal layer microstructure and the arrangement of algal cells within this layer. These are difficult tasks in a harsh environment.

Implications for primary production—Sea ice is composed of a matrix of pure ice with brine, gas, and absorbing constituents trapped in interstices between and within the substructure of ice crystals (Fig. 3). The scattering and absorption properties of sea ice are dependent upon constituent volume fractions and their structural arrangement (Ehn et al. 2008*a*). It has been suggested and supported by values reported in the literature that in situ bottom ice algal absorption of solar irradiance may be greater than laboratory measurements of in vivo absorption (Smith et al. 1988; Perovich et al. 1993). We suggest that this discrepancy stems from an artifact of comparing radiation absorption by cells in a highly scattering environment to that in seawater or a melted ice sample. The effect of scattering, which is to increase the pathlength of photons propagating in the sea ice, thereby increasing the probability of photons being absorbed, can explain this difference. The increase in photon pathlength due to scattering is not a new concept. For example, it represents a difficulty in calibration of the quantitative filter technique for in vivo absorption measurements (Mitchell et al. 2003). In the atmosphere, multiple scattering due to aerosols can greatly increase the effective absorption optical depth by, e.g., gases (Ben-David 1997; Mayer et al. 1998). Furthermore, coral skeletons have been shown to enhance absorption by symbiotic algae (Enríquez et al. 2005).

To examine the potential effect of absorption amplification on primary production estimates in the sea ice bottom algal layer, the new parameter, Φ, was added to the *P-E* formula (Platt et al. 1980), assuming no photoinhibition:

$$P^B_{\mathrm{apparent}} = P^B_{\max}\left[1 - e^{-\left(\bar{E}_0 \alpha^B \Phi / P^B_{\max}\right)}\right] \qquad (11)$$

where P^B_{apparent} is the apparent Chl *a*–specific photosynthetic rate that is adjusted to the light levels within the bottom sea ice environment (mg C mg Chl a^{-1} h^{-1}), $P^B_{\max}$ is the light-saturated Chl *a*–specific photosynthetic rate (mg C mg Chl a^{-1} h^{-1}), and α^B is the Chl *a*–specific photosynthetic efficiency (mg C mg Chl a^{-1} h^{-1} [μmol m^{-2} s^{-1}]$^{-1}$). The Φ values added here were those described earlier with $\mu_{\mathrm{d}} = 0.7$, $\mu_{\mathrm{u}} = 0.5$, $b_{\mathrm{tot}} = 165.3$ m^{-1}, and $R_{top}(500) = 4\%$. It is stressed that Eq. 11 be interpreted as an apparent *P-E*

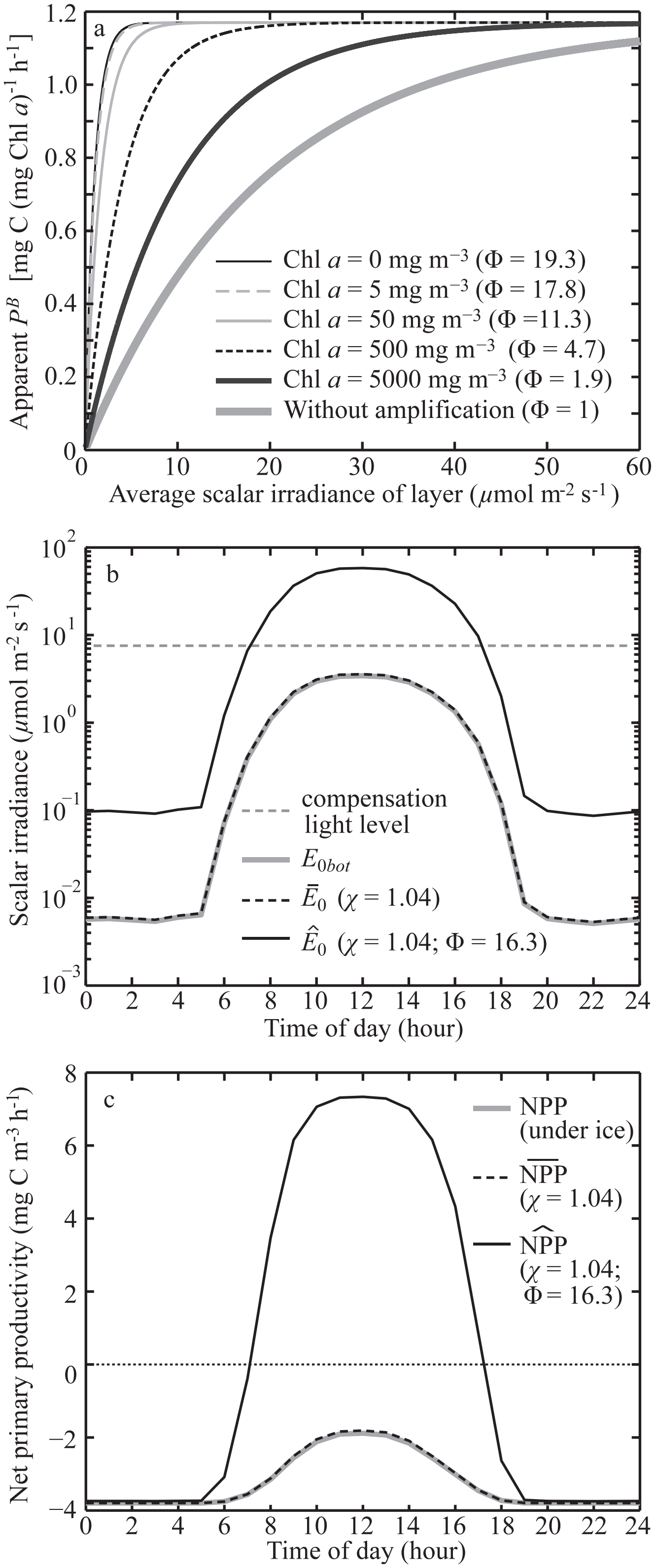

Fig. 7. (a) The predicted response of adjusting a *P-E* relationship to the absorption amplification factor, Φ, calculated over a range of ice algal Chl *a* concentrations. The *P-E* relationship was estimated using averaged values of $P^B_{\max}$ = 1.17 mg C mg Chl a^{-1} h^{-1} and α^B = 0.061 mg C mg Chl a^{-1} h^{-1} (μmol m^{-2} s^{-1})$^{-1}$ obtained from laboratory measurements presented in Smith et al. (1988). (b) Early spring (pre-bloom) diurnal response of estimated bottom ice scalar irradiance, and (c) net primary production to layer average opacity, χ, and pathlength amplification, Φ, for a Chl *a* of 10 mg m^{-3} (*see* Discussion).

←

relationship and should not be confused with the interpretation that algal physiology changes due to the addition of Φ, i.e., algal physiological parameters can only be derived from a *P-E* curve obtained in non-scattering media.

The effect of adding Φ, i.e., using $\hat{E}_0$ rather than $\overline{E}_0$, in the exponent of Eq. 11 was to increase the initial slope of the P^B_{apparent} function such that higher photosynthetic rates were reached at significantly lower $\overline{E}_0$ levels than suggested without consideration of absorption amplification due to scattering, particularly for low Chl *a* with high Φ (Fig. 7a). The apparent light-limited production was also shifted to a much lower $\overline{E}_0$ range. As a consequence, *P-E* relationships would predict a greater degree of light limitation of photosynthesis in situ when the in situ irradiance estimate does not consider scattering. This would result in an underestimation of primary production, affecting the timing and magnitude of modeled biological productivity.

The influence of scattering on primary production in sea ice was further explored through a simple modeling exercise to estimate bottom ice net primary production over a diurnal period. During the 2004 Canadian Arctic Shelf Exchange Study, pre-bloom ice algal biomass was between 0.02 and < 1.16 mg m^{-2} in the bottom 4 cm of the ice cover, with the bloom commencing mid- to late March under > 0.1 m deep snow covers (Różańska et al. 2009). Measurements on 18 March showed that 0.5% of the incident PAR was transmitted through the snow and ice cover. To estimate $E_{\mathrm{d}bot}$(PAR) over a diurnal cycle in pre-bloom conditions, we multiplied this transmittance value by diurnal (1-h time step) surface incident PAR data from the same study site and averaged over a 5-d period (16 to 20 March 2004). Equations 7, 9, and 10 were used to calculate E_{0bot}, $\overline{E}_0$, and $\hat{E}_0$, respectively (Fig. 7b). For these calculations, χ and Φ were estimated using a Chl *a* of 10 mg m^{-3} (0.25 mg m^{-2} over a 2.5 cm sea ice layer). The physiological *P-E* relationship used in Fig. 7a, i.e., where $\Phi = 1$, was applied to estimate gross primary production for E_{0bot}, $\overline{E}_0$, and $\hat{E}_0$. Finally, net primary production (NPP) was estimated assuming an ice algae compensation light intensity of 7.6 μmol m^{-2} s^{-1} (Gosselin et al. 1985). Figure 7c shows that in sub-ice waters and in sea ice without consideration of scattering, NPP would be negative throughout the diurnal period, whereas it is positive in sea ice when adjusted to $\hat{E}_0$. Dividing the compensation light intensity by Φ, which was 16.3 at a Chl *a* of 10 mg m^{-3}, provides an apparent compensation level of 0.47 μmol m^{-2} s^{-1}. Interestingly, this apparent estimate is consistent with the in situ sea ice study of Mock and Gradinger (1999), who observed positive NPP to occur at an averaged 0.36 μmol m^{-2} s^{-1}, providing support for the significant role of absorption amplification on NPP in sea ice.

Following this comparison, these results also highlight that *P-E* relationships measured in situ could result in faulty parameter approximations, unless E_0 is properly determined for the ice algae. Furthermore, a significant underestimation of ice algal production is expected when using sub-ice primary production incubations to directly estimate ice algal production where water column scattering is low relative to sea ice. Therefore, current ice algal primary production estimates may need to be revisited in lieu of results presented here. Our results imply that the most representative primary production estimates would be based on net irradiance measurements combined with spectrally corrected *P-E* parameters from incubations in which scattering effects would be small and irradiance levels are well defined.

Enhanced radiation absorption in high-scattering environments also provides a useful theory to further explain algal phenology in the springtime polar marine ecosystem. Barring advection of allochthonous biomass (Robinson et al. 1995), the concentration of phytoplankton in the water column is typically low under an ice algal community (Gosselin et al. 1997). However, in the Antarctic, while phytoplankton biomass remained small (< 0.1 mg Chl *a* m^{-3}), platelet ice and benthic algal communities were documented to shade-acclimate below a bottom ice algal community (Robinson et al. 1995), provided it takes an investment of energy and time for algae to photoacclimate (Falkowski and Raven 2007). These three communities all exist within or on high-scattering media and could therefore have a significant advantage over phytoplankton for establishing communities under low light conditions and earlier in the season. Similarly, when transmitted irradiance levels increase during ice melt, too much light absorption could induce photoinhibition of sea ice algal communities, providing an advantage for phytoplankton production in the water column at this time.

Acknowledgments

This work began when J. K. Ehn was supported through postdoctoral fellowships from the Centre National d'Études Spatiales (CNES) and from the National Aeronautics and Space Administration (NASA) Cryosphere Program Award NNX07AR20G and C. J. Mundy by a Fonds "Québécois de la recherche sur la nature et les technologies" postdoctoral fellowship. We thank two anonymous reviewers, and all those who reviewed early versions, for suggestions and comments that significantly improved the paper. This paper is a contribution to the research programs of ArcticNet and the Centre for Earth Observation Science at the University of Manitoba.

References

ARRIGO, K. R., J. N. KREMER, AND C. W. SULLIVAN. 1993. A simulated Antarctic fast ice ecosystem. J. Geophys. Res. **98:** 6929–6946, doi:10.1029/93JC00141

———, C. W. SULLIVAN, AND J. N. KREMER. 1991. A bio-optical model of Antarctic sea ice. J. Geophys. Res. **96:** 10581–10592, doi:10.1029/91JC00455

BEN-DAVID, A. 1997. Multiple-scattering effects on differential absorption for the transmission of a plane-parallel beam in a homogeneous medium. Appl. Opt. **36:** 1386–1398, doi:10.1364/AO.36.001386

COMISO, J. C., C. L. PARKINSON, R. GERSTEN, AND L. STOCK. 2008. Accelerated decline in the Arctic sea ice cover. Geophys. Res. Lett. **35:** L01703, doi:10.1029/2007GL031972

EHN, J. K., C. J. MUNDY, AND D. G. BARBER. 2008*a*. Bio-optical and structural properties inferred from irradiance measurements within the bottommost layers in an Arctic landfast sea ice cover. J. Geophys. Res. **113:** C03S03, doi:10.1029/2007JC004194

———, T. N. PAPAKYRIAKOU, AND D. G. BARBER. 2008*b*. Inference of optical properties from radiation profiles within melting landfast sea ice. J. Geophys. Res. **113:** C09024, doi:10.1029/2007JC004656

Enríquez, S., E. R. Méndez, and R. Iglesias-Prieto. 2005. Multiple scattering on coral skeletons enhances light absorption by symbiotic algae. Limnol. Oceanogr. **50:** 1025–1032, doi:10.4319/lo.2005.50.4.1025

Falkowski, P. G., and J. A. Raven. 2007. Aquatic photosynthesis, 2nd ed. Princeton Univ. Press.

Gosselin, M., L. Legendre, S. Demers, and R. G. Ingram. 1985. Responses of sea-ice microalgae to climatic and fortnightly tidal energy inputs (Manitounuk Sound, Hudson Bay). Can. J. Fish. Aquat. Sci. **42:** 999–1006, doi:10.1139/f85-125

———, M. Levasseur, P. A. Wheeler, R. A. Horner, and B. C. Booth. 1997. New measurements of phytoplankton and ice algal production in the Arctic Ocean. Deep-Sea Res. II **44:** 1623–1644, doi:10.1016/S0967-0645(97)00054-4

Grenfell, T. C. 1979. The effects of ice thickness on the exchange of solar radiation over the polar oceans. J. Glaciol. **22:** 305–320.

———, and D. K. Perovich. 1981. Radiation absorption coefficients of polycrystalline ice from 400 to 1400 nm. J. Geophys. Res. **86:** 7447–7450, doi:10.1029/JC086iC08p07447

Henyey, L. G., and J. L. Greenstein. 1941. Diffuse radiation in the galaxy. Astrophys. J. **93:** 70–83, doi:10.1086/144246

Kirk, J. T. O. 1994. Estimation of the absorption and the scattering coefficients of natural waters by use of underwater irradiance measurements. Appl. Opt. **33:** 3276–3278, doi: 10.1364/AO.33.003276

Kirst, G. O., and C. Wiencke. 1995. Ecophysiology of polar algae. J. Phycol. **31:** 181–199, doi:10.1111/j.0022-3646.1995.00181.x

Kühl, M., R. N. Glud, J. Borum, R. Roberts, and S. Rysgaard. 2001. Photosynthetic performance of surface-associated algae below sea ice as measured with a pulse-amplitude-modulated (PAM) fluorometer and O_2 microsensors. Mar. Ecol. Prog. Ser. **223:** 1–14, doi:10.3354/meps223001

Lavoie, D., K. Denman, and C. Michel. 2005. Modeling ice algal growth and decline in a seasonally ice-covered region of the Arctic (Resolute Passage, Canadian Archipelago). J. Geophys. Res. **110:** C11009, doi:10.1029/2005JC002922

Light, B., T. C. Grenfell, and D. K. Perovich. 2008. Transmission and absorption of solar radiation by Arctic sea ice during the melt season. J. Geophys. Res. **113:** C03023, doi:10.1029/2006JC003977

Maffione, R. A. 1998. Theoretical developments on the optical properties of highly turbid waters and sea ice. Limnol. Oceanogr. **43:** 29–33, doi:10.4319/lo.1998.43.1.0029

Manes, S. S., and R. Gradinger. 2009. Small scale vertical gradients of Arctic ice algal photophysiological properties. Photosynth. Res. **102:** 53–66, doi:10.1007/s11120-009-9489-0

Maritorena, S., A. Morel, and B. Gentili. 1994. Diffuse reflectance of oceanic shallow waters: Influence of water depth and bottom albedo. Limnol. Oceanogr. **39:** 1689–1703, doi:10.4319/lo.1994.39.7.1689

Maslanik, J. A., C. Fowler, J. Stroeve, S. Drobot, J. Zwally, D. Yi, and W. Emery. 2007. A younger, thinner Arctic ice cover: Increased potential for rapid extensive sea-ice loss. Geophys. Res. Lett. **34:** L24501, doi:10.1029/2007GL032043

Mayer, B., A. Kylling, S. Madronich, and G. Seckmeyer. 1998. Enhanced absorption of UV radiation due to multiple scattering in clouds: Experimental evidence and theoretical explanation. J. Geophys. Res. **103:** 31241–31254, doi:10.1029/98JD02676

McMinn, A., C. Ashworth, and K. G. Ryan. 2000. In situ net primary productivity of an Antarctic fast ice bottom algal community. Aquat. Microb. Ecol. **21:** 177–185, doi:10.3354/ame021177

Mitchell, B. G., M. Kahru, J. Wieland, and M. Stramska. 2003. Determination of spectral absorption coefficients of particles, dissolved material and phytoplankton for discrete water samples, p. 39–64. *In* G. S. Fargion, J. L. Mueller, and C. R. McClain [eds.], Ocean optics protocols for satellite ocean color sensor validation. NASA Technical Memorandum 2003-211621/Rev4-Vol. IV. National Aeronautical and Space Administration, Goddard Space Flight Center, Greenbelt, Maryland.

Mock, T., and R. Gradinger. 1999. Determination of Arctic ice algal production with a new in situ incubation technique. Mar. Ecol. Prog. Ser. **177:** 15–26, doi:10.3354/meps177015

Morel, A., and S. Maritorena. 2001. Bio-optical properties of oceanic waters: A reappraisal. J. Geophys. Res. **106:** 7163–7180, doi:10.1029/2000JC000319

Mundy, C. J., J. K. Ehn, D. G. Barber, and C. Michel. 2007. Influence of snow cover and algae on the spectral dependence of transmitted irradiance through Arctic landfast first-year sea ice. J. Geophys. Res. **112:** C03007, doi:10.1029/2006JC003683

———, and others. 2011. Characteristics of two distinct high-light acclimated algal communities during advanced stages of sea ice melt. Polar Biol. **34:** 1869–1886, doi:10.1007/s00300-011-0998-x

Nishi, Y., and S. Tabeta. 2005. Analysis of the contribution of ice algae to the ice-covered ecosystem in Lake Saroma by means of a coupled ice–ocean ecosystem model. J. Mar. Syst. **55:** 249–270, doi:10.1016/j.jmarsys.2004.08.002

Ohlmann, J. C., D. A. Siegel, and C. D. Mobley. 2000. Ocean radiant heating. Part I: Optical influences. J. Phys. Oceanogr. **30:** 1833–1848, doi:10.1175/1520-0485(2000)030<1833:ORHPIO>2.0.CO;2

Perovich, D. K. 1990. Theoretical estimates of light reflection and transmission by spatially complex and temporally varying sea ice covers. J. Geophys. Res. **95:** 9557–9567, doi:10.1029/JC095iC06p09557

———, G. F. Cota, G. A. Maykut, and T. C. Grenfell. 1993. Bio-optical observations of first-year arctic sea ice. Geophys. Res. Lett. **20:** 1059–1062, doi:10.1029/93GL01316

Platt, T., C. L. Gallegos, and W. G. Harrison. 1980. Photoinhibition of photosynthesis in natural assemblages of marine phytoplankton. J. Mar. Res. **38:** 687–701.

Ralph, P. J., A. McMinn, K. G. Ryan, and C. Ashworth. 2005. Short-term effect of temperature on the photokinetics of microalgae from the surface layers of Antarctic pack ice. J. Phycol. **41:** 763–769, doi:10.1111/j.1529-8817.2005.00106.x

Robinson, D. H., K. R. Arrigo, R. Iturriaga, and C. W. Sullivan. 1995. Microalgal light-harvesting in extreme low-light environments in McMurdo Sound, Antarctica. J. Phycol. **31:** 508–520, doi:10.1111/j.1529-8817.1995.tb02544.x

Różańska, M., M. Gosselin, M. Poulin, J. M. Wiktor, and C. Michel. 2009. Influence of environmental factors on the development of bottom ice protist communities during the winter–spring transition. Mar. Ecol. Prog. Ser. **386:** 43–59, doi:10.3354/meps08092

Smith, R. E. H., J. Anning, P. Clement, and G. Cota. 1988. Abundance and production of ice algae in Resolute Passage, Canadian Arctic. Mar. Ecol. Prog. Ser. **48:** 251–263, doi: 10.3354/meps048251

———, P. Clément, and E. Head. 1989. Biosynthesis and photosynthate allocation patterns of arctic ice algae. Limnol. Oceanogr. **34:** 591–605, doi:10.4319/lo.1989.34.3.0591

Welch, H. E., and M. A. Bergmann. 1989. Seasonal development of ice algae and its prediction from environmental factors near Resolute, N.W.T., Canada. Can. J. Fish. Aquat. Sci. **46:** 1793–1804, doi:10.1139/f89-227

Associate editor: Heidi M. Sosik

Received: 24 August 2012
Accepted: 28 January 2013
Amended: 30 January 2013